Supplementary Information

Single-Particle Optical Study on the Effect of Chloride Post-treatment of $MAPbI_3$ Nanocrystals

Handong Jin [#a], Amitrajit Mukherjee [#a], Lata Chouhan [a], Julian A. Steele [b,d], Flip de Jong [a], Yujie Gao [b], Maarten B. J. Roeffaers [b], Johan Hofkens *[a, c] and Elke Debroye *[a]

[a]Department of Chemistry, KU Leuven, Celestijnenlaan 200F, Leuven, Belgium

[b]cMACS, Department of Microbial and Molecular Systems, KU Leuven, 3001 Leuven, Belgium

[c]Max Planck Institute for Polymer Research, Ackermannweg 10, 55128 Mainz, Germany

[d]School of Mathematics and Physics, The University of Queensland, Brisbane, QLD, 4072, Australia

Correspondence to:

E-mail: johan.hofkens@kuleuven.be; elke.debroye@kuleuven.be

Supplementary Figures

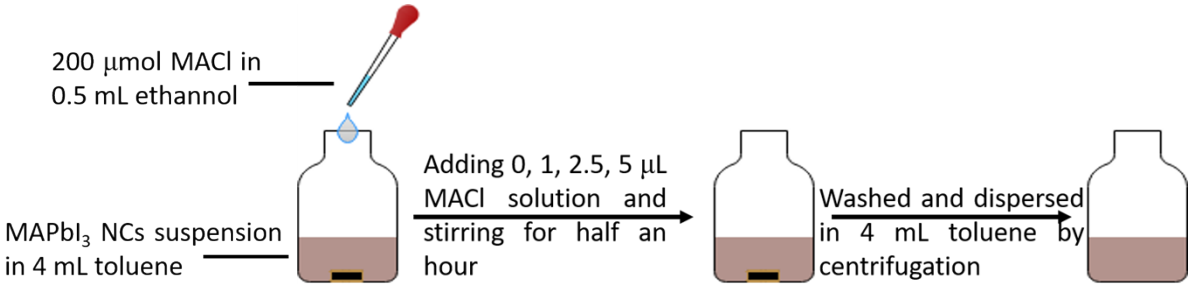

Fig. S1. Schematic representation of MACl post-treatment of $MAPbI_3$ NCs.

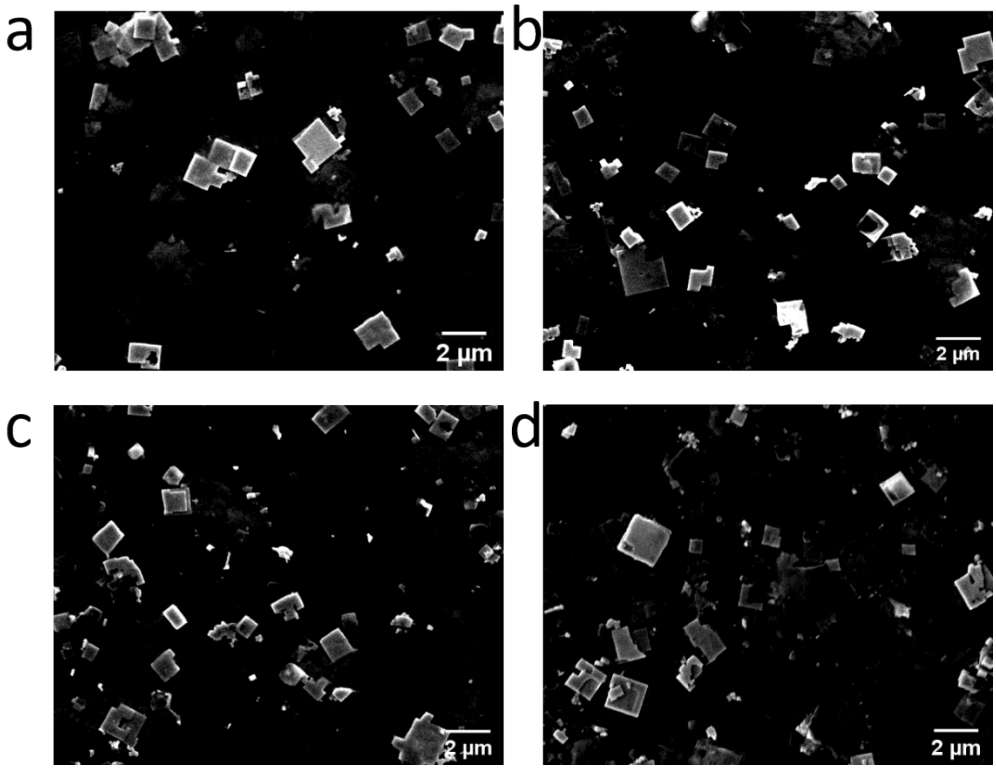

Fig. S2. SEM images of (a) $MAPbI_3$, (b) $MAPbI_3$-3%Cl, (c) $MAPbI_3$-9%Cl and (d) $MAPbI_3$-17%Cl NCs.

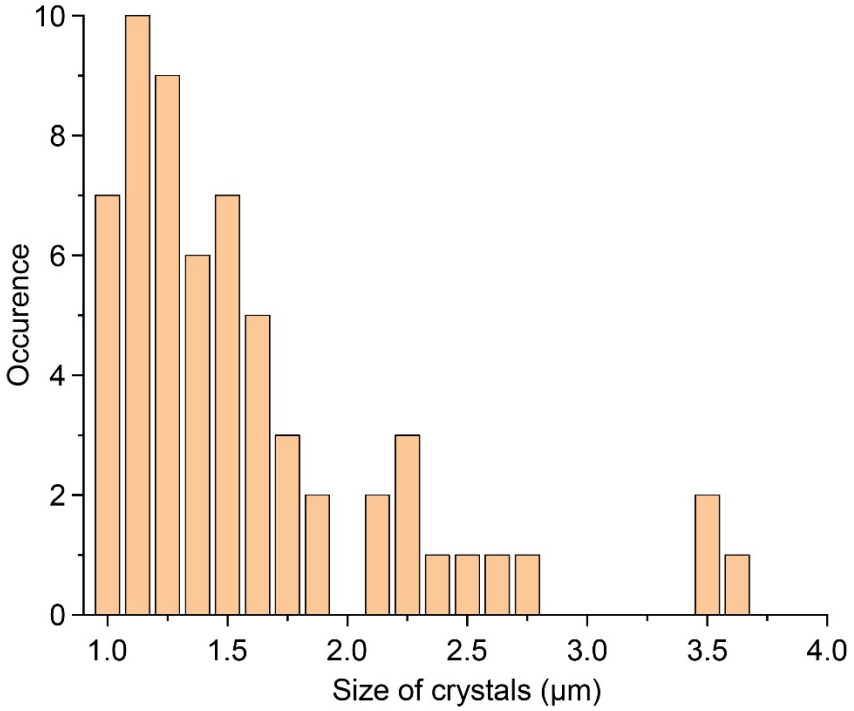

Fig. S3. Size distribution of the (un)passivated $MAPbI_3$ microcrystals population.

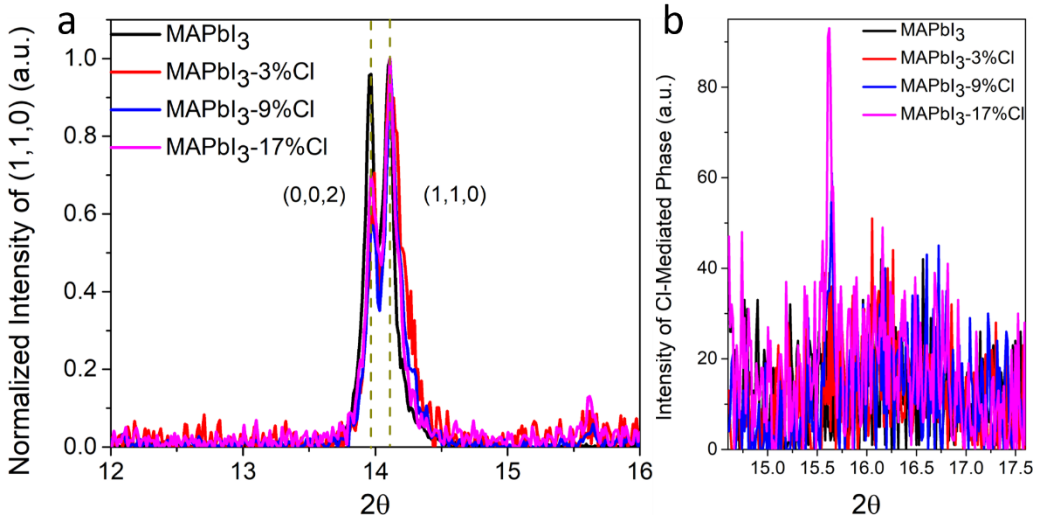

Fig. S4 (a) Comparison of (002) and (110) Bragg peaks. (b) Zoom out of XRD pattern at around 15.6 º of $MAPbI_3$, $MAPbI_3$-3%Cl, $MAPbI_3$-9%Cl and $MAPbI_3$-17%Cl NCs. It is shown that the diffraction peak at 15.6 º begin to appear for $MAPbI_3$-9%Cl NCs and becomes stronger for $MAPbI_3$-17%Cl NCs.

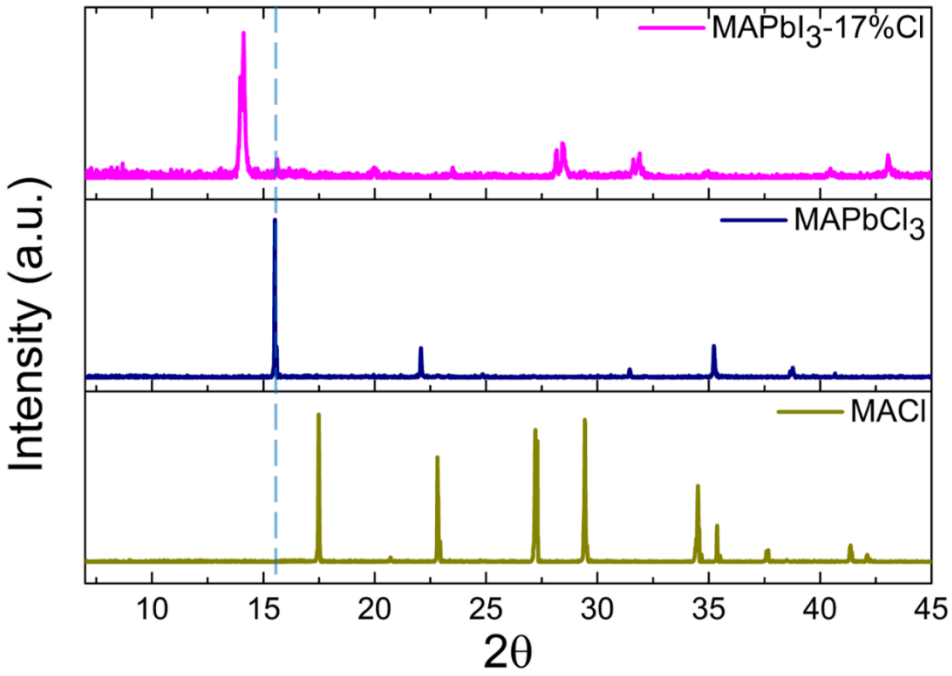

Fig. S5. XRD patterns of $MAPbI_3$-17%Cl NCs, $MAPbCl_3$ and MACl thin films. Apparently, the peaks at 15.6 º originate from the formation of $MAPbCl_3$.

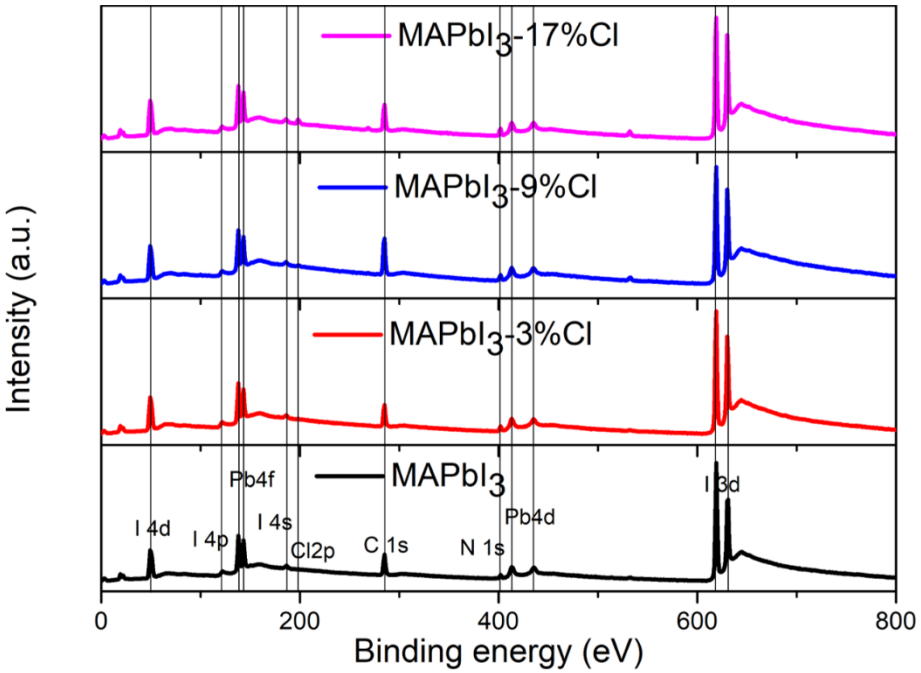

Fig. S6. XPS survey spectra of $MAPbI_3$, $MAPbI_3$-3%Cl, $MAPbI_3$-9%Cl and $MAPbI_3$-17%Cl NCs.

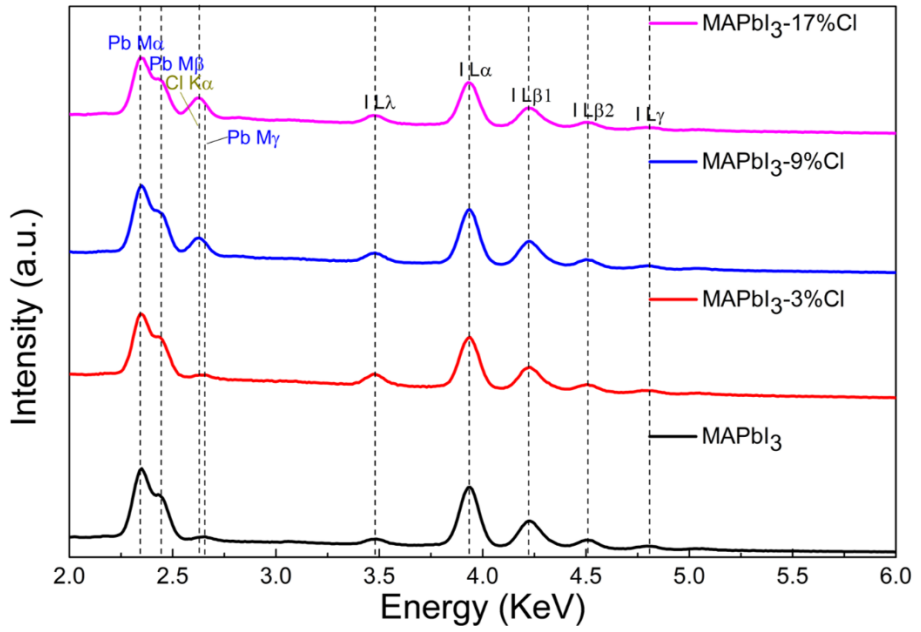

Fig. S7. EDS spectra and elemental composition (inset) of $MAPbI_3$, $MAPbI_3$-3%Cl, $MAPbI_3$-9%Cl and $MAPbI_3$-17%Cl NCs.

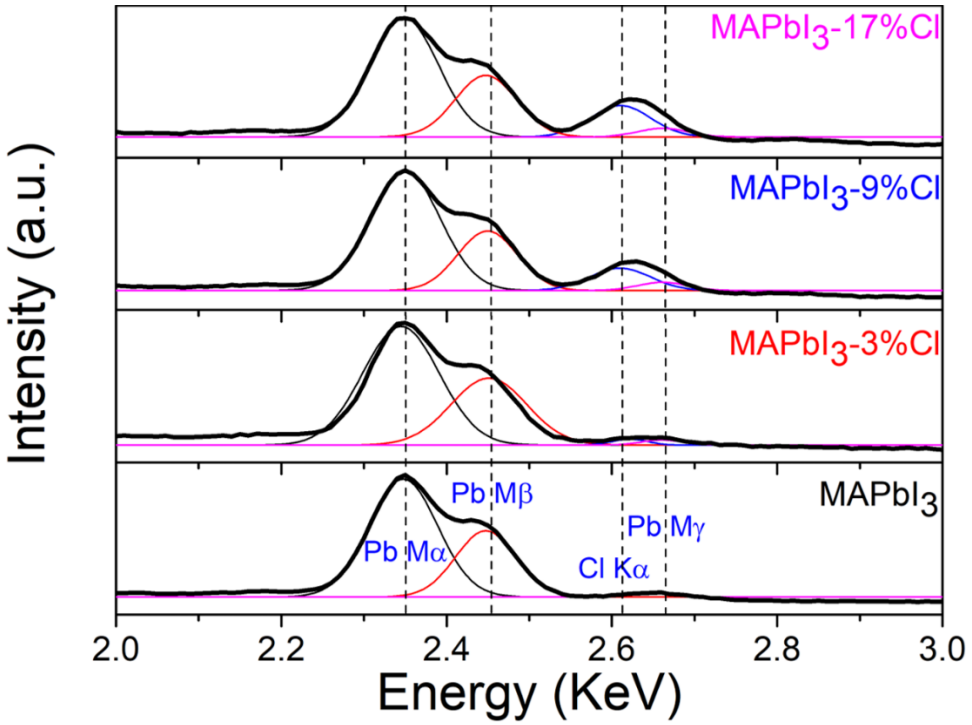

Fig. S8. Fitted EDS spectra of $MAPbI_3$, $MAPbI_3$-3%Cl, $MAPbI_3$-9%Cl and $MAPbI_3$-17%Cl NCs. The content of chloride gradually increases with the amount of MACl added.

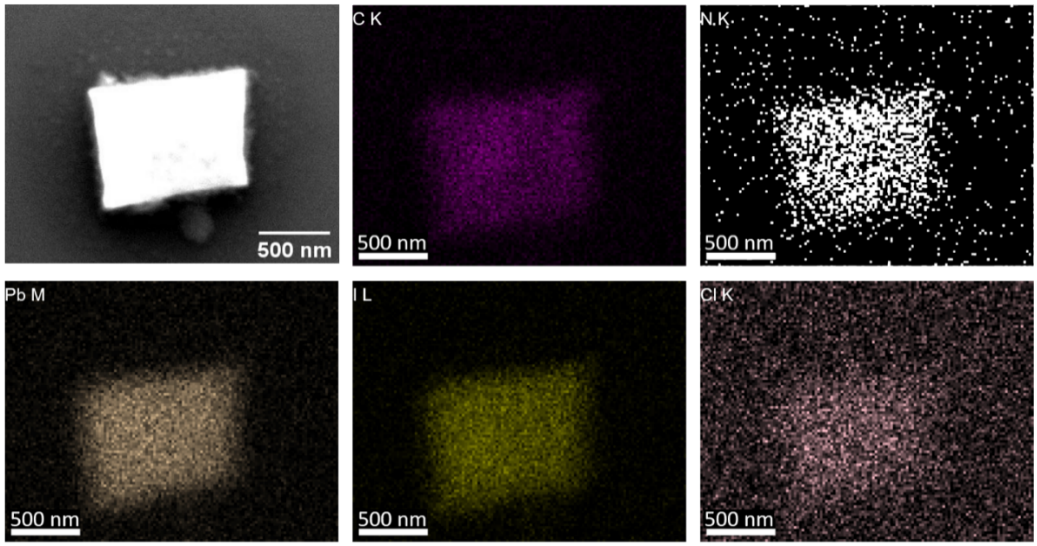

Fig. S9. EDS mapping of carbon, nitrogen, lead, iodide and chloride elements for $MAPbI_3$-3%Cl NCs.

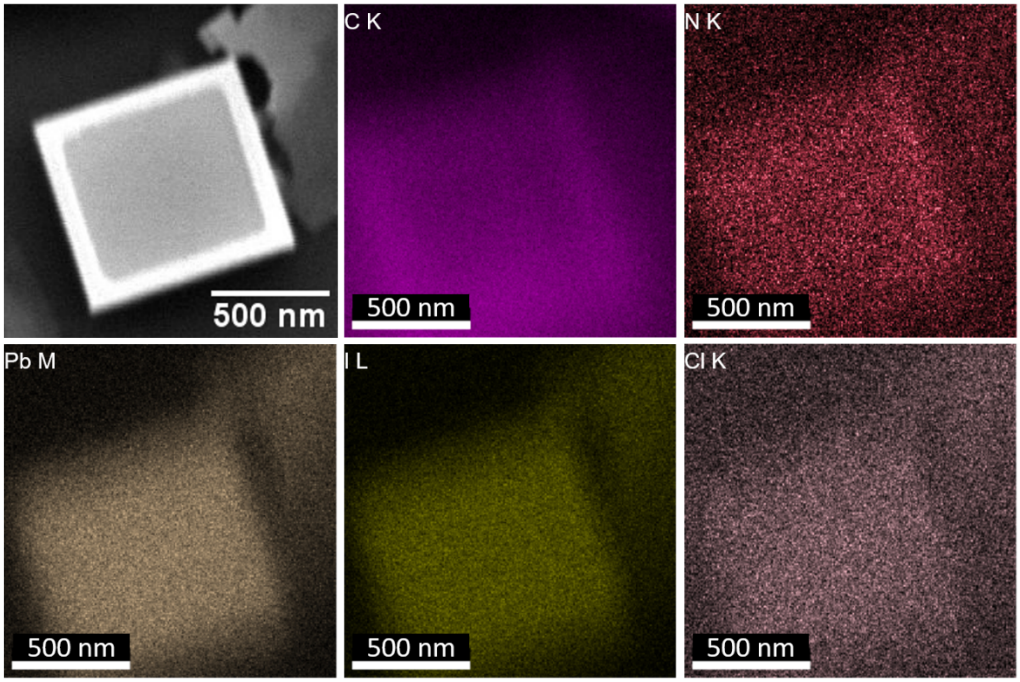

Fig. S10. EDS mapping of carbon, nitrogen, lead, iodide and chloride elements for $MAPbI_3$-9%Cl NCs.

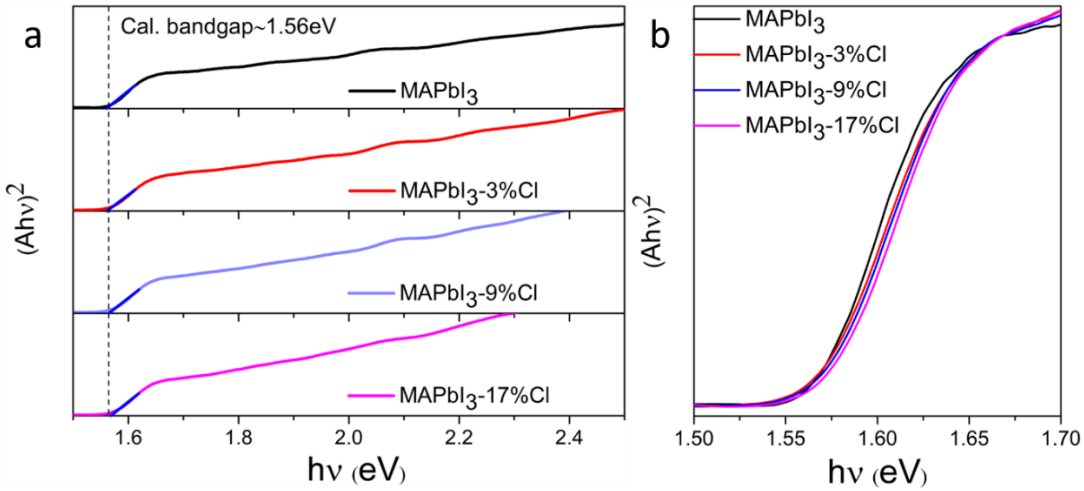

Fig. S11. (a) Tauc plots of $MAPbI_3$, $MAPbI_3$-3%Cl, $MAPbI_3$-9%Cl, and $MAPbI_3$-17%Cl. The bandgap energies were estimated after Kubelka-Munk transformation.[1] Each bandgap is determined by the intersection point of the corresponding dashed tangent line and horizontal axis. (b) Zoom out of Tauc plots of untreated and post-treated $MAPbI_3$ NCs. Although the calculated bandgap keep almost the same, a slightly larger bandgap with showing blue shift can be observed.

The PLQY values show an evolution of 1.1%, over 1.4% and 1.6% to 3.2% (excitation power density: 0.9 $mWcm^{-2}$) for the pure $MAPbI_3$ NCs, the $MAPbI_3$-3%Cl, $MAPbI_3$-9%Cl, and $MAPbI_3$-17%Cl post-treated NCs, respectively. The relatively low PLQY values compared with literature originate from the relatively large size of the NCs. [2 2] Interestingly, a slight PL blue shift (~2 nm) is found after 3% Cl treatment. A blue or redshift of emission wavelengths is attributed to a change

of the electronic structure in the band tail states. Because the band tail states are governed by structural disorder or defects in NCs, they usually exhibit a redshift in the PL spectrum edge. Defect passivation by chloride treatment reduces the band tail states in the bandgap and thus leads to a slightly blue shift of PL emission. Therefore, the blue shift in the PL spectrum, along with the PL enhancement, probably originate from the remediation of traps (in the band tail states).

Further blue-shifts of PL peak position with increasing Cl content, are related to the shift of band edges. The shift of the band edges has usually been attributed to the charge transfer between the passivating compound and the perovskite surface. Especially, Zheng et al. reported that $MAPbI_3$ perovskite films with a passivated surface exhibit a slightly larger bandgap compared to non-passivated perovskites.[3] Similarly, in our work, upon formation of $MAPbCl_3$ on the crystal surface when adding 9% to 17% Cl, a further blue-shift (~6 nm) of PL peaks can be observed due to the large bandgap of $MAPbCl_3$. although all the Cl untreated and treated NCs show almost the same bandgap (1.56eV), the NCs with Cl-passivated surfaces exhibit a slightly gradual larger bandgap compared with the pristine $MAPbI_3$ NCs as shown in Fig. S11.

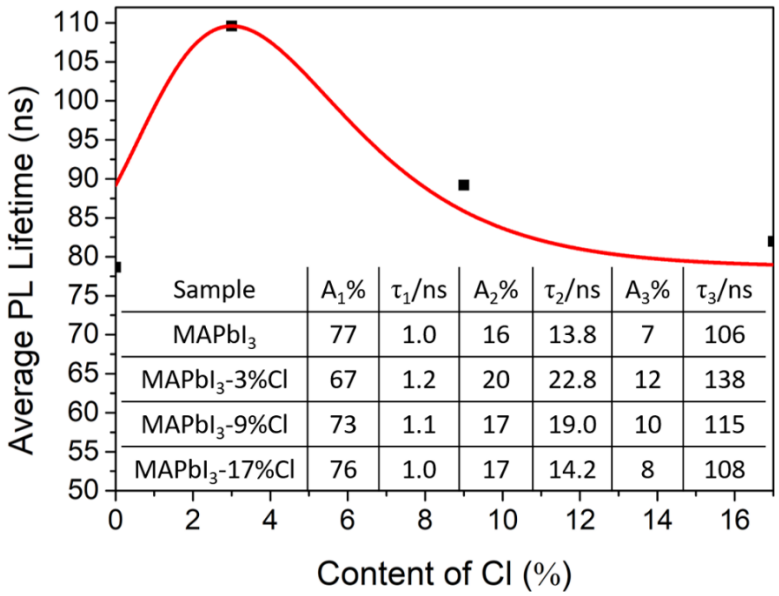

Sample	A_1%	τ_1/ns	A_2%	τ_2/ns	A_3%	τ_3/ns
$MAPbI_3$	77	1.0	16	13.8	7	106
$MAPbI_3$-3%Cl	67	1.2	20	22.8	12	138
$MAPbI_3$-9%Cl	73	1.1	17	19.0	10	115
$MAPbI_3$-17%Cl	76	1.0	17	14.2	8	108

Fig. S12. Variation on the averaged PL lifetime extracted from the fitted PL decay curves (fitted parameters depicted in the inset table).

Analysis of time-correlated single-photon counting (TCSPC) data

In order to deeply understand the dynamics of the photo-generated carriers in the perovskite nanoparticles, we recorded the TCSPC histograms of the $MAPbI_3$ NCs without and with the Cl post-treatment. Single or double exponential functions cannot describe the decay curves. The TCSPC data could be fitted by a triple-exponential decay function as shown in the following equation:

$$I(t) = A_1 \exp\left(\frac{-t}{\tau_1}\right) + A_2 \exp\left(\frac{-t}{\tau_2}\right) + A_3 \exp\left(\frac{-t}{\tau_3}\right) + B$$

Where A_1, A_2, A_3, τ_1, τ_2, τ_3 and B are the decay amplitudes, the decay lifetimes, and a constant for the baseline offset (noise), respectively.

The average decay time $\bar{\tau}$ () in Fig. S12 was calculated according to the formula

$$\bar{\tau} = (A_1\tau_1^2 + A_2\tau_2^2 + A_3\tau_3^2)/(A_1\tau_1 + A_2\tau_2 + A_3\tau_3)$$

The fitting results are listed in the inset table of Fig. 2b.

When the content of MACl further increases, with the appearance of a tiny amount of $MAPbCl_3$ phase as shown in the XRD spectra, the long lifetime components of the fitted curves of the NCs with 9% and 17%Cl treatment gradually decrease, suggesting less freedom for the diffusion of the free charge carriers and thus again, relatively high trap densities compared with that of the 3%Cl-treated $MAPbI_3$ NCs.

Table S1. A brief comparison of the lifetime components before and after halide-based doping or post-treatment of $MAPbI_3$ (-based) materials.

Publication	MHP system under study	Chemicals used for MAX (X = Cl, I) treatment	Remarks
Method: Cl-doping			
Jin et al. Adv. Opt. Mater.*, 2021, 9, 2002240** ***(Ref. 15 in ms)	**$MAPbI_3$ nanocrystals**	**MACl was dissolved in pure DMSO and directly added to the precursor solution**	**PL lifetime was fitted with a tri-exponential function. Lifetime increased with increasing extent of Cl-doping.** **1. Pristine: τ_1 = 0.55 ns, τ_2 = 5.26 ns, τ_3 = 50.5 ns** **2. 2% Cl-doping: τ_1 = 0.78 ns, τ_2 = 9.64 ns, τ_3 = 90.8 ns** **3. 5% Cl-doping: τ_1 = 1.15 ns, τ_2 = 16.18 ns, τ_3 = 108 ns**
Saidaminov et al. Nat. Energy 2018, 3, 648–654. ***(Ref. 17 in ms)***	**$Cs_{0.05}MA_{0.15}FA_{0.8}$-$PbI_{2.55}Br_{0.45}$ film**	**$PbCl_2$ added in the precursor (CsMAFA) solution in DMSO + DMF (1:4) maintaining a 5% Cl concentration**	**Improved stability of Cl-treated perovskites. Improved PL lifetime (bi-exponential) after Cl-treatment.** **Pristine CsMAFA: τ_1 = 11 ns, τ_2 = 877 ns** **Cl-treated: τ_1 = 12 ns, τ_2 = 954 ns** **Variation of the PL lifetime with the concentration of MACl is not reported.**
Son et al. Nat. Energy 2016, 1, 16081 ***(Ref. 16 in ms)***	**$MAPbI_3$ film**	**An excess of MAI is used in the precursor solution in DMSO as,**	**Bi-exponential fitting** **1. τ_1 = 3.4 – 3.89 ns and τ_2 = 15.7-18.6 ns**

		1. MAI:PbI_2 = 0.9:1 to 1:1 **2. MAI:PbI_2 = 1.06:1** **3. MAI:PbI_2 = 1.1:1**	**2. τ_1 = 3.9, τ_2 = 24.9 ns** **3. τ_1 = 1.7, τ_2 = 12.8 ns** **Enhancement of lifetime upon usage of excess MAI. However, a high excess of MAI (MAI:PbI_2 = 1.1:1) creates new defects and deteriorates the PL lifetime.**
Method: Cl-based post-treatment			
Aristidou et al. Nat. Commun. 2017, 8, 15218. ***(Ref. 19 in ms)***	**$MAPbI_3$ film**	**Salts: MAI and MACl in IPA + chloro-benzene (1:4)**	**The stability in presence of light and oxygen increases after MAI post-treatment. Increasing amounts of MAI increased the PL lifetime.** **1. Lifetime components are not separately compared.** **2. MACl-post-treated $MAPbI_3$ undergoes material degradation as compared to the pristine material.** **3. A critical extent of passivation has not been investigated.**
Hwang et al. J. Appl. Phys. 2019, 126, 023101. ***(Ref. 13 in ms)***	**$MAPbI_3$ film**	**Salt: 9 mM MACl in ethanol + cyclohexane (1:3)** **Remark: No other concentrations of MACl were tested.**	**PL intensity and lifetime increase after the post-treatment.** **1. Lifetime components are not separately compared.** **2. Variation of the PL lifetime with the concentration of MACl is not reported.** **3. A critical extent of passivation has not been investigated.**
Kogo et al. Chem. Commun., 2020, 56, 1235 ***(Ref. 18 in ms)***	**$Cs_{0.05}(FA_{0.83}MA_{0.17})_{0.95}$ –$Pb(I_{0.83}Br_{0.17})_3$ film**	**MACl, MABr, MAI, FAI solution in isopropanol was directly spin-coated on the $Cs_{0.05}(FA_{0.83}MA_{0.17})_{0.95}$ – $Pb(I_{0.83}Br_{0.17})_3$ film**	**No information on the PL lifetime has been reported.**
Jin et al. ***(Present work)***	**$MAPbI_3$ nano and microcrystals**	**3% (low), 9% (moderate), 17% (high) MACl post-treatment in ethanol/toluene mixed solvent (v/v ratios are 0.025%, 0.065% and 0.125%)**	**1. Longer PL lifetime can be achieved using a controlled (~3%) MACl treatment.** **2. PL lifetime decreases in case of moderate (9%) and excessive (17%) MACl treatment, indicating deterioration of the material quality and**

			formation of new defects at $MAPbCl_3/I_3$ heterojunctions. **3. PL lifetime components have been analyzed and compared.** **<u>Pristine</u>: τ_1 = 1.0 ns, τ_2 = 13.8 ns, τ_3 = 106 ns** **<u>3% Cl</u>: τ_1 = 1.2 ns, τ_2 = 22.8 ns, τ_3 = 138 ns**

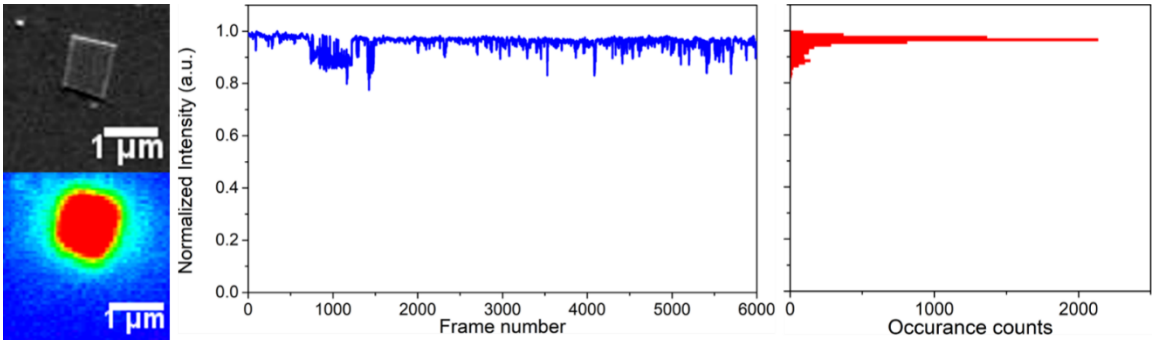

Fig. S13. SEM and PL images of a single "blinking-free" $MAPbI_3$ NC with 3%Cl surface treatment.

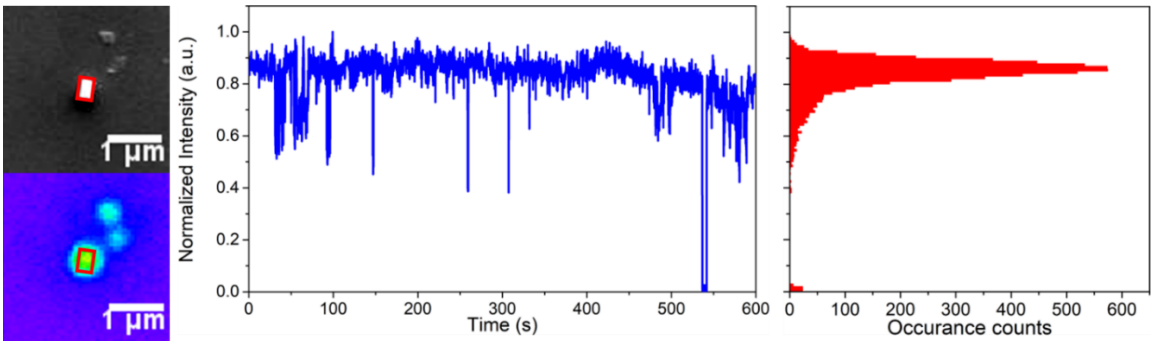

Fig. S14. SEM and PL images of a single $MAPbI_3$ NC with 9%Cl surface treatment (shown by the red square).

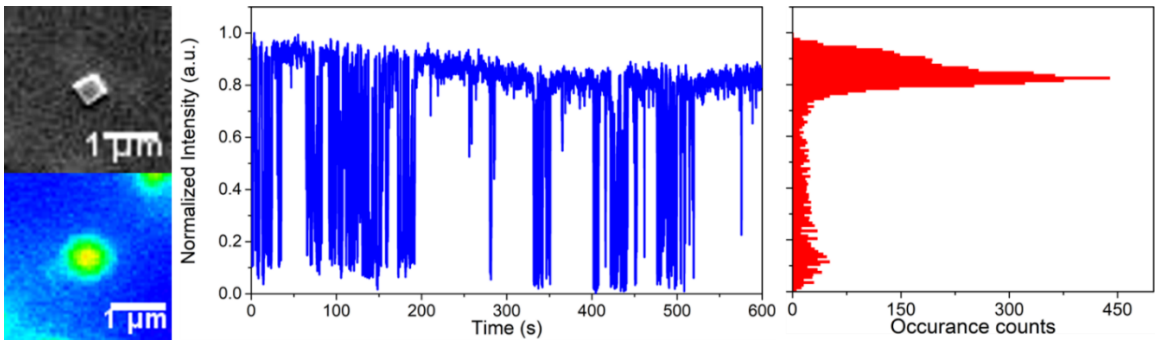

Fig. S15. SEM and PL images of a single $MAPbI_3$ NC with 17%Cl surface treatment.

For the majority $MAPbI_3$-3%Cl crystals, clear suppression of blinking with the appearance of blinking-free trajectories, can be observed (Fig. S13). This is in agreement with the increased PL lifetime, also suggesting reduced trap densities. However, with higher MACl content, the blinking frequency starts to increase again, indicating an additional trap density increase, as shown in Fig. S14 and Fig. S15. Note that the blinking frequency of $MAPbI_3$-17%Cl post-treated is almost similar to that of the pristine $MAPbI_3$ NCs.

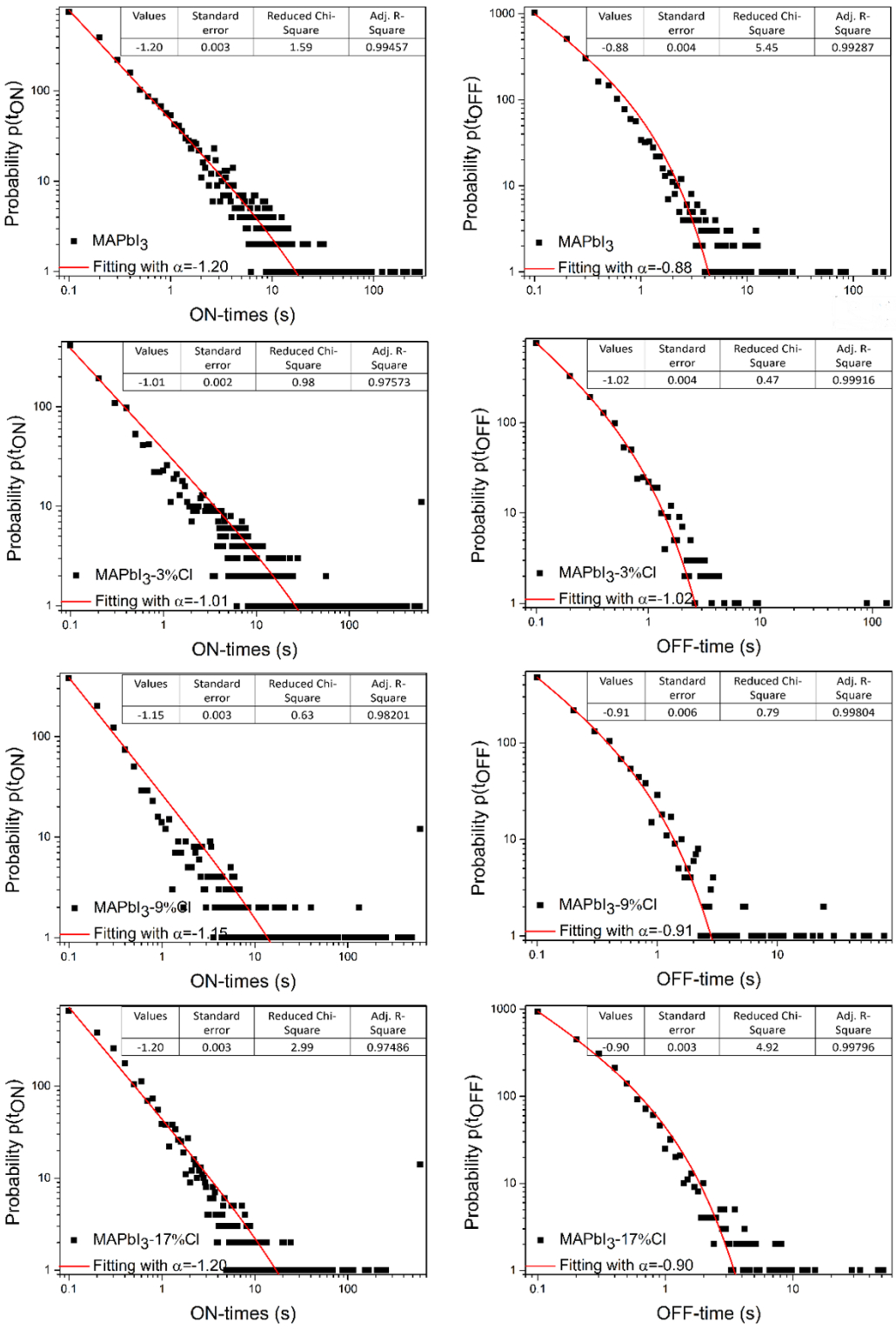

Fig. S16. Power-law fitting parameters for the probability distributions of the duration of ON times and OFF times of $MAPbI_3$ NCs with 0, 3, 9, and 17%Cl surface treatment.

Note 1: The power-law exponents of ON states decreased again from α= -1.15 to -1.20 for $MAPbI_3$ with 9% and 17%Cl treatment, respectively. Meanwhile, lower power-law exponents of OFF states were obtained around -0.90 for pure $MAPbI_3$-9%Cl and $MAPbI_3$-17%Cl post-treated NCs, respectively. After the appearance of the $MAPbCl_3$ phase, blinking frequency begin to increase again, even though higher PL intensity values were obtained possibly due to the band offset of $MAPbI_3$ and $MAPbCl_3$. (more explanation in Fig, S22)

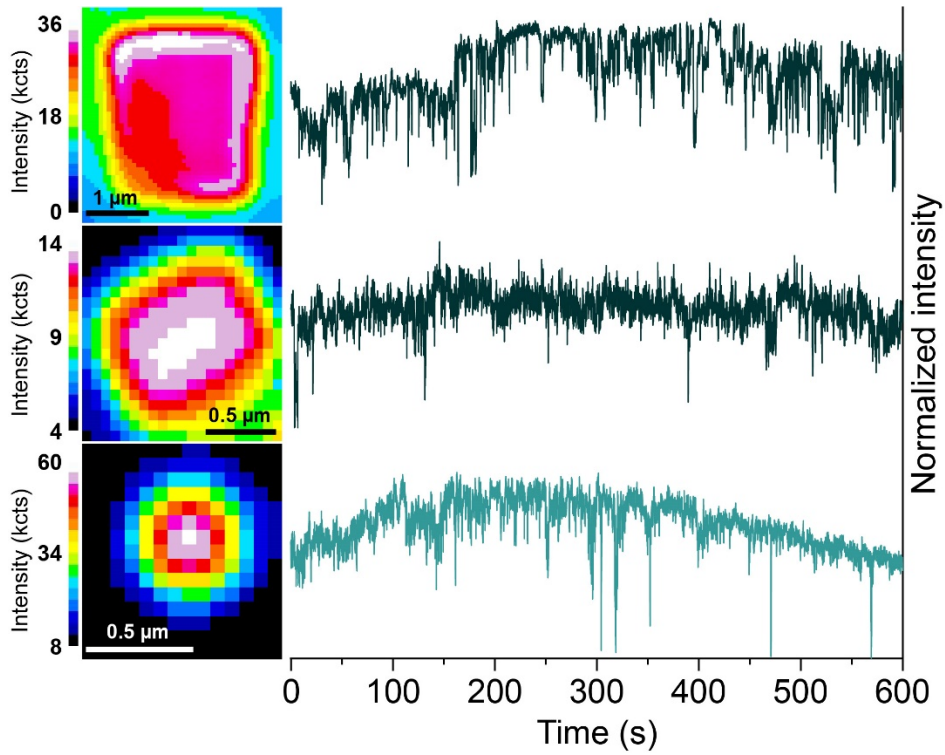

Fig. S17. Brightening-bleaching-blinking (*BBB*) characteristic of three representative micro and nanocrystals are demonstrated (top to bottom).

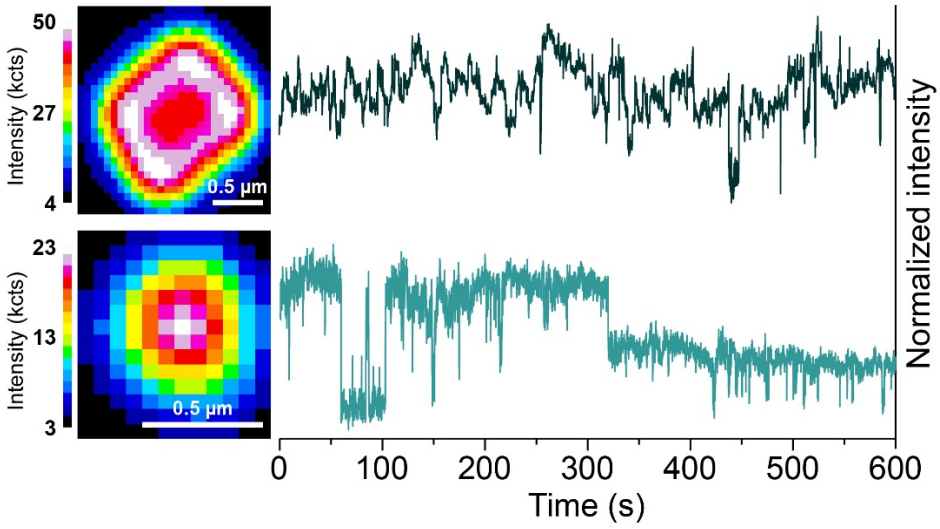

Fig. S18. Two representative micro and nanocrystals are shown with their multi-states blinking (*MSB*) nature.

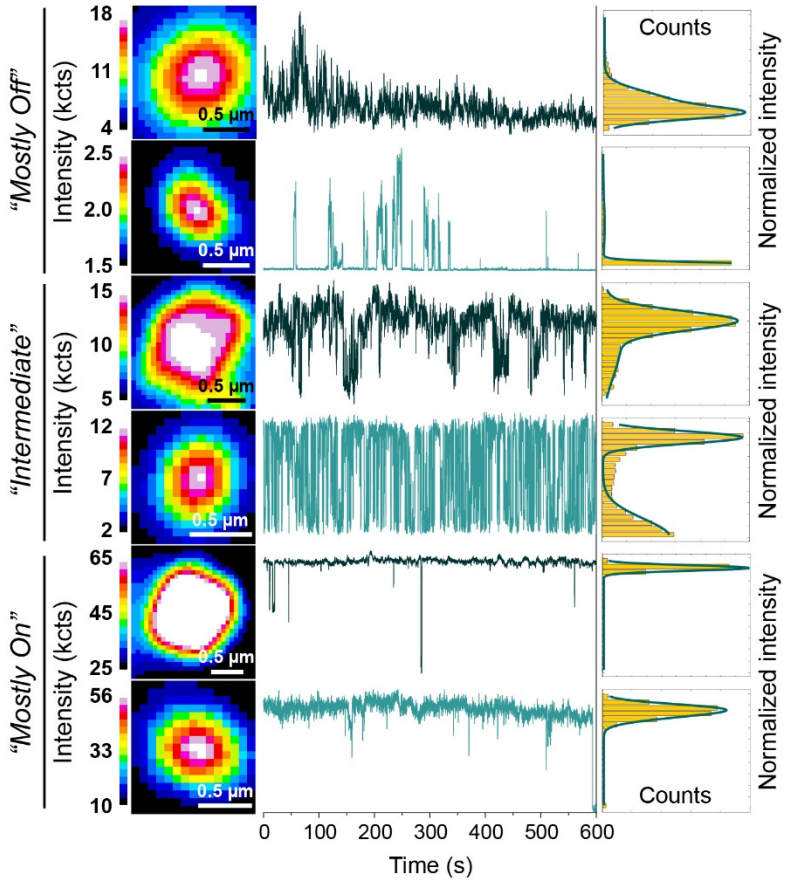

Fig. S19. Three classes of blinking characteristics, "*Mostly Off*", "*Intermediate*" and "*Mostly On*", are shown (top to bottom) for the representative micro and nanocrystals. Intensity distributions (fitted with double Gaussian function) of each blinking trajectory are shown (yellow) in the right panel.

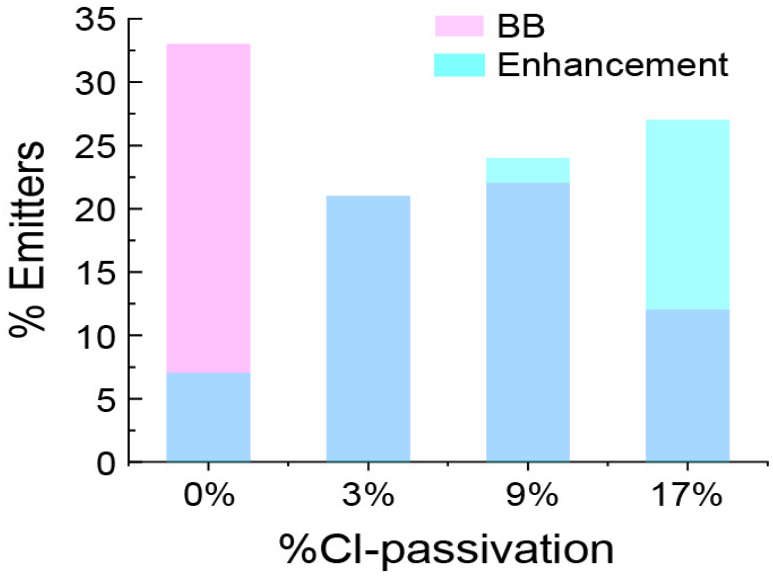

Fig. S20. Bar-charts comparison of the emitter occurrence statistics of *BB* (pink) and *PEB* (cyan) characteristic before and after different extent of Cl-based passivation. Dark blue part of the chart represents the overlapped section.

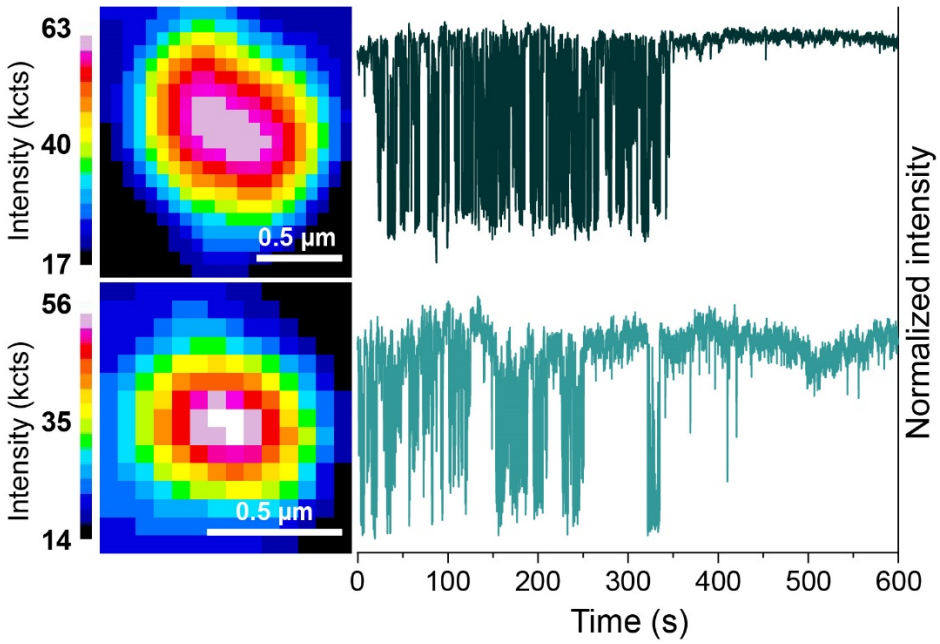

Fig. S21. Two representative micro and nanocrystals (passivated) showing blinking suppression under photo-irradiation.

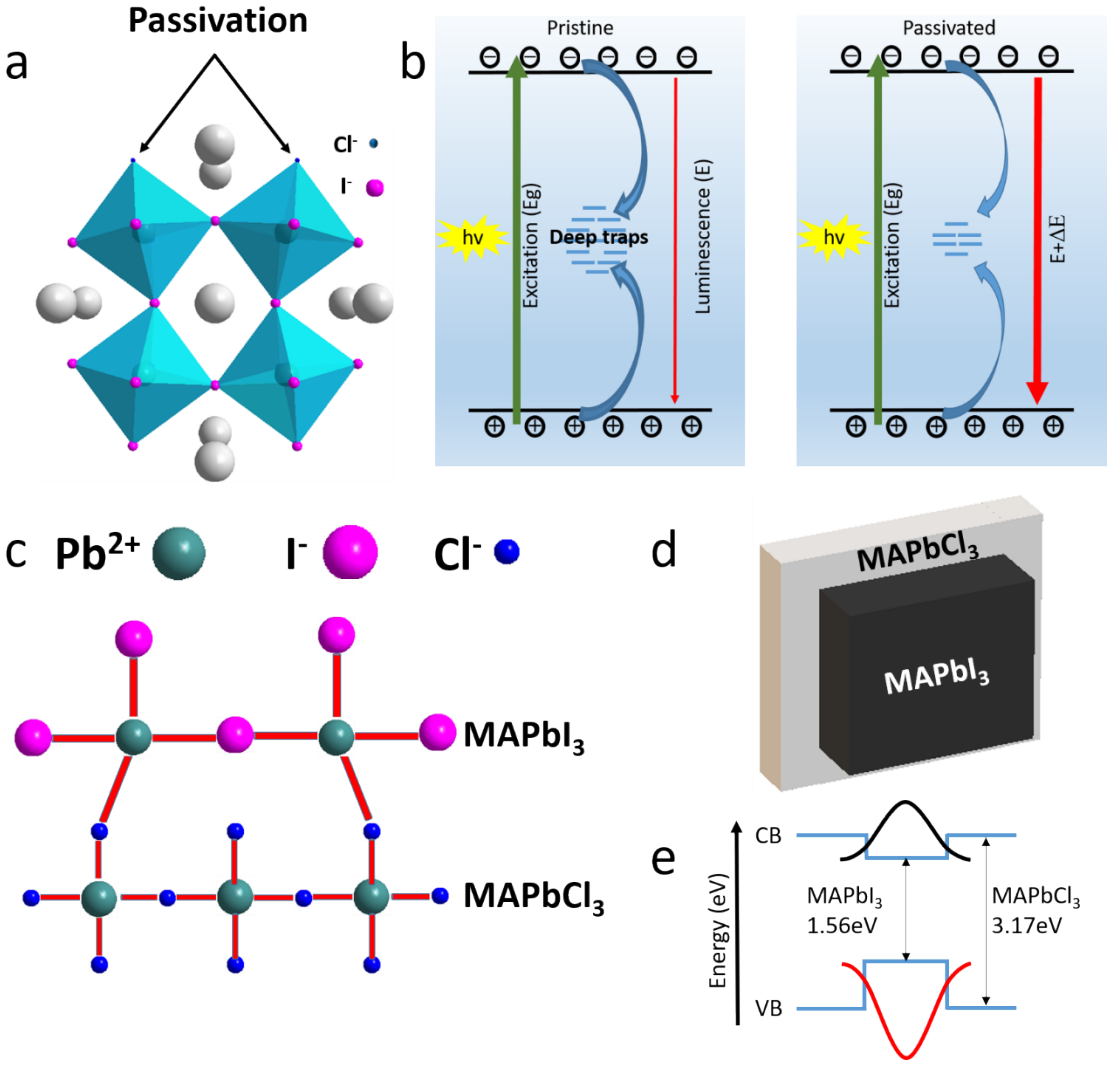

Fig. S22. Schematic illustration showing (a) replacement of iodide vacancies by chloride ions. The grey, black, pink, and blue spheres represent MA cation, Pb, I, and Cl elements, respectively. (b) The effect of MACl post-treatment on the electronic traps in $MAPbI_3$ NCs. Schematic illustration showing (c) Mismatch between $MAPbI_3$ and $MAPbCl_3$. (d) $MAPbI_3/MAPbCl_3$ core/shell structure. (e) Band alignment in $MAPbI_3/MAPbCl_3$ core/shell NCs. CB and VB represent the conduction and valence band; E_g of 1.56 eV and E_g of 3.17 eV are the bandgaps of $MAPbI_3$ and $MAPbCl_3$, respectively.

Note 2: When the $MAPbCl_3$ structure is formed on the $MAPbI_3$ NC surface for $MAPbI_3$-9%Cl and $MAPbI_3$-17%Cl NCs, the mismatch between these two perovskite structures may create new surface defects on the $MAPbI_3$ NCs or at their interface, resulting in relatively higher blinking frequencies. Quantum wells are generated in layered hetero-structures by joining different semiconductor materials.[4, 5] Our characterization results imply that the emitting $MAPbI_3$ bulk (1.56

eV) becomes partially coated by a thin layer of $MAPbCl_3$ with a large bandgap (3.17 eV) upon excessive Cl-treatment, generating a two-layered semiconductor heterostructure with a quantum well band structure of $MAPbI_3$ residing in the $MAPbCl_3$ bandgap, (so-called Type-I heterojunction). In the core $MAPbI_3$, the conduction band energy is lower, and the valence band energy is higher, as illustrated in Fig. S22.[6] Therefore, both electrons and holes can be confined in the $MAPbI_3$ region, resulting in a fast exciton decay rate and hence higher PLQY values. A similar phenomenon was reported in a $CsPbBr_3/Cs_4PbBr_6$ core/shell structure.[6] The higher quantum efficiency is expected to further result in a higher probability of switching to OFF states in the PL blinking trajectory. Hence, higher blinking frequencies and related fast PL decays agree with the higher PLQY values in the core/shell NCs upon excessive MACl post-treatment.

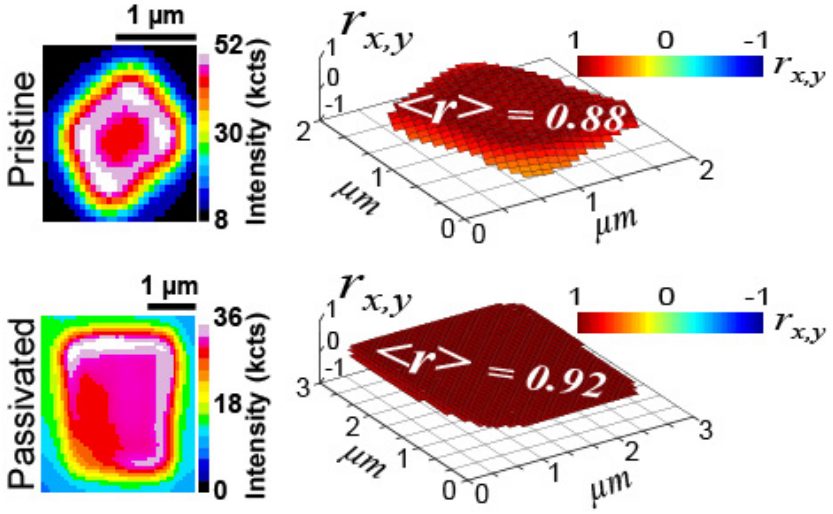

Fig. S23. Depiction of correlation maps for the representative $MAPbI_3$ MCs before (upper panel) and after MACl post-treatment (lower panel).

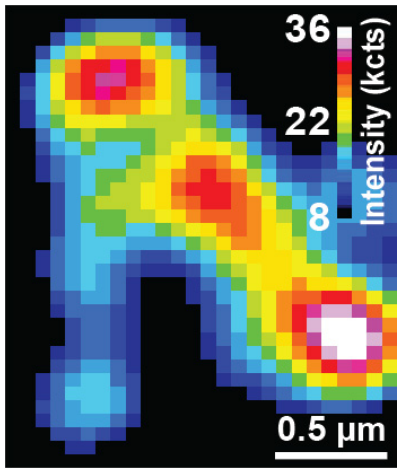

Fig. S24. PL microscopy image representing the self-assembly of $MAPbI_3$ NCs on the glass coverslip.

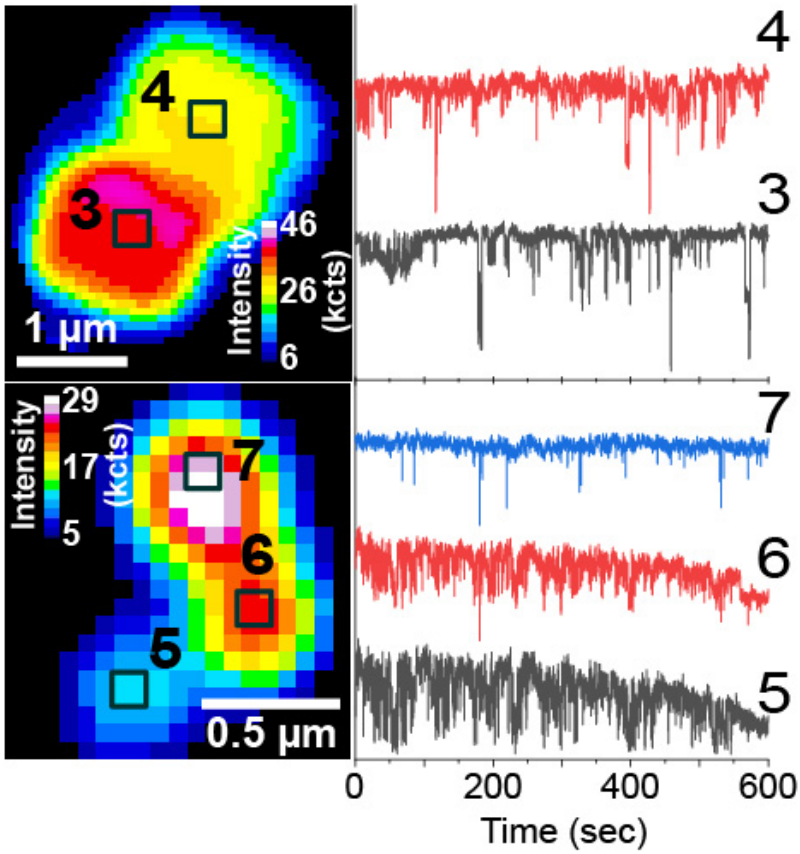

Fig. S25. Photoluminescence intermittency of the spatially separated regions of an assembly of two MCs (upper panel) and three NCs (lower panel).

References

1. P. Makuła, M. Pacia and W. Macyk, *Journal*, 2018, **9**, 6814-6817.
2. I. G. Scheblykin, *Adv. Energy Mater.*, 2020, **10**, 2001724.
3. X. Zheng, B. Chen, J. Dai, Y. Fang, Y. Bai, Y. Lin, H. Wei, X. C. Zeng and J. Huang, *Nat. Energy*, 2017, **2**, 1-9.
4. D. A. Miller, *Quantum Dynamics of Simple Systems," ed. G.-L. Oppo, SM Barnett, E. Riis, and M. Wilkinson (Institute of Physics, London, 1996)*, 1994, 239-226.
5. H. Kumar, A. Kumari and R. R. Singh, *Opt. Mater.*, 2017, **69**, 23-29.
6. C. Jia, H. Li, X. Meng and H. Li, *Chem. Commun.*, 2018, **54**, 6300-6303.